Mapping the targetable proteome of metastatic castration-resistant prostate cancer

<u>Authors</u>: Mikhail Dias^{1, 2#}, Chien-Kuang Cornelia Ding^{1, 3,}, Sophie Déglise^{7, 8}, Stefanie Engler⁷, Helen Richards¹¹, Erolcan Sayar¹¹, Aishwarya Subramanian¹, Adam Foye¹, Shuang G. Zhao¹⁵, Joshua M. Lang¹⁵, Peter R. Carroll^{1, 4}, Eric J. Small^{1, 6}, Rahul Aggarwal⁶, Colm Morrissey¹⁴, David A. Quigley^{1, 4, 5}, Peter S. Nelson^{11, 13}, Felix Y. Feng^{1, 2, 5}, Michael C. Haffner^{9, 11, 12}, Bernd Bodenmiller^{7, 8}, William S. Chen^{1, 2}

Affiliations: ¹Helen Diller Family Comprehensive Cancer Center, University of California San Francisco, San Francisco, CA; ²Department of Radiation Oncology, UCSF, San Francisco; ³Department of Pathology, University of California, San Francisco, San Francisco, CA, ⁴Department of Epidemiology and Biostatistics, UCSF, San Francisco, CA; ⁵Department of Urology, UCSF, San Francisco, CA; ⁶Department of Hematology and Oncology, Department of Medicine, University of California, San Francisco, San Francisco, CA; ⁷Department of Quantitative Biomedicine, University of Zurich, Zurich, Switzerland; ⁸Institute of Molecular Health Sciences, ETH Zurich, Zurich, Switzerland; ⁹Department of Laboratory Medicine and Pathology, University of Washington, Seattle, WA; ¹¹Division of Human Biology, Fred Hutchinson Cancer Research Center, Seattle, WA; ¹³Division of Hematology and Oncology, Department of Medicine, University of Washington, Seattle, WA; ¹⁴Department of Urology, University of Washington, Seattle, WA; ¹⁵Department of Medicine, University of Wisconsin-Madison, Madison, WI; *presenter

Background: Metastatic castration-resistant prostate cancer (mCRPC) is a leading cause of cancer-related mortality in men across the world. Despite recent advances in therapies, treatment resistance remains a hurdle, largely attributed to intra- and inter-tumoral heterogeneity. Single-cell characterization of the targetable molecular and histologic features of mCRPC across tissue sites is critical for optimizing therapeutic strategies.

Methods: 181 metastatic prostate cancer tumour biopsies from 58 patient autopsies were obtained and measured on the Imaging Mass Cytometry (IMC) platform using a custom prostate cancer-specific panel enriched for targetable tumor markers including PSMA, CD46, AR, KLK2, and STEAP1. The published 'steinbock' approach was used to segment cells and quantify protein expression at single-cell resolution. Cell subtypes were defined using the Phenograph cell-clustering approach. Per-sample "cell fraction" (percent abundance) of each cell subtype was defined as cell count of that subtype divided by total number of cells in the sample. Clinical data, including pathology annotations of tumor subtypes using conventional tumor profiling approaches, were collected to interrogate genomic features associated with known clinicopathologic features of interest. Differences in cell counts across metastatic sites were assessed using a Chi-square test at a significance level of 0.05.

Results: IMC performed on 1,623,494 cells from mCRPC tumours revealed 35 distinct cell populations including adenocarcinoma, neuroendocrine (NE), immune, and stromal cells (Figure 1A-C). Cell fraction analysis (relative quantification of all cell subtypes within each tumour) was consistent with pathologist-annotated tumour subtypes, including AR+/NE- and AR-/NE+ disease as defined based on conventional pathology assays (Figure 1D). Amongst most patients with multiple tumour biopsies, tumours exhibited consistent cellular compositions across metastatic sites. However, a small subset of patients (10%) demonstrated intertumoral heterogeneity, defined as presence of at least two tumours with distinct predominant cancer cell subtypes. AR and PSMA were more frequently co-expressed in lymph node than in liver tumour cells (87% vs 58%, P<0.05). Furthermore, CD46, a targetable cell-surface tumour marker, was more frequently co-expressed with AR in LN tumour cells (85%) than in bone (64%), lung (65%), or liver (66%) tumour cells (P<0.05), suggestive of metastatic organotropism and potentially different biological drivers based on metastatic site.

<u>Conclusions</u>: Using a custom prostate cancer-specific single-cell assay, we characterized intra- and inter-tumoral heterogeneity based on targetable tumor marker co-expression patterns. Observed differences in cancer cell enrichment patterns by metastatic site highlight the importance of single cell approaches paired with robust clinical annotations to account for potential confounders associated with advanced disease. Additional studies are needed to validate promising drug targets and treatment combinations.

<u>Funding Acknowledgements:</u> This study was supported by a PCF TACTICAL Award (01TACT23) and PCF Young Investigator Award (24YOUN07).

<u>Conflicts of Interest</u>: CKCD has received research funding from Bristol Myers Squibb and Intuitive Surgical. CM has received funds from Genentech and Novartis. PSN served as a paid advisor for Bristol Myers Squibb, Pfizer, Genentech, AstraZeneca, and Janssen. MCH served as a paid consultant/received honoraria from Pfizer and AstraZeneca and has received research funding from Merck, Novartis, Genentech, Promicell, and Bristol Myers Squibb. BB is a co-founder, shareholder, and board member of Navignostics and is a member of the scientific advisory board of Standard BioTools.

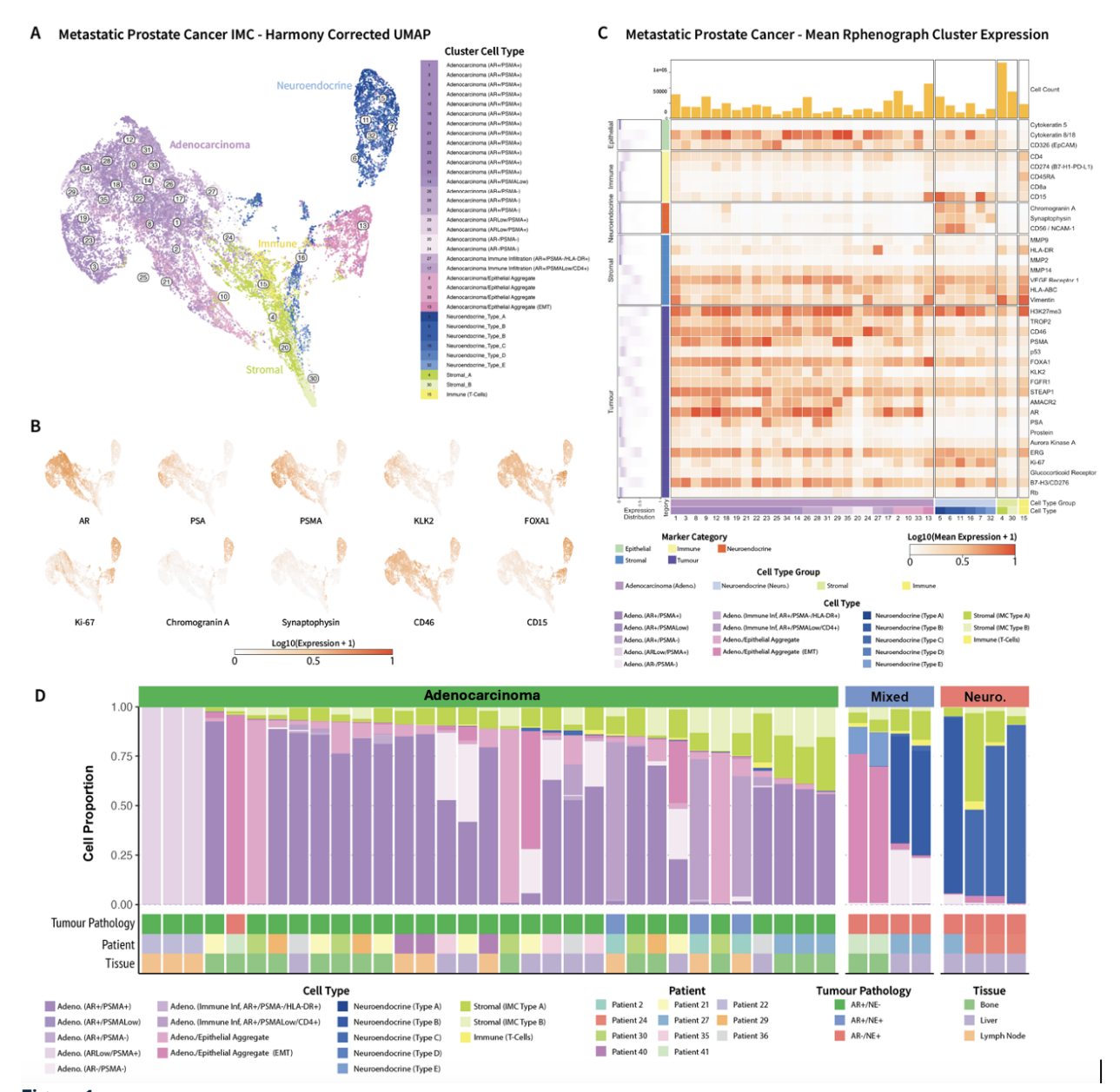


Figure 1.

- A UMAP dimensionality reduction plot showing distinct single-cell subtypes defined by protein co-expression patterns measured using IMC.
- B-UMAP dimensionality reduction plot of cell subtypes, with each cell (point) colored by log-normalized protein expression of selected protein markers.
- C Heatmap of mean protein expression of each measured protein (rows) for each single-cell subtype (columns). Bar plot (above heatmap) represents total cell count (abundance) of each cell subtype. IMC-derived cell subtypes (1-35) corresponding to cell subtype IDs shown in Figure 1A are annotated below the heatmap.
- D Cell fraction bar plot of samples profiled using IMC and annotated by expert pathologist using paired H&E and immunohistochemistry (IHC) slides. Colors in stacked bar plot denote IMC-derived cell subtypes (legend below). Tumor samples (columns) were defined as adenocarcinoma, mixed, or neuroendocrine based on per-sample cell fractions of adenocarcinoma and neuroendocrine cell subtypes. Expert pathology annotations (based on H&E and IHC findings), patient ID, and tissue site of origin for each sample are shown below the stacked bar plots.